ISSN: 2664-9640

# Research and Optimization of Axial Superconducting Bearing

Luqi Han [1], Xiaochen Ren [2],Hang Yan[1]

[1] School of Chengdu University of Technology, Chengdu 610000, China;

[2] School of Hebi Automotive Engineering Professional College, Hebi 458030, China.

## Abstract

**High-temperature Superconducting Magnetic Bearing can work at higher speeds without active control, and can simultaneously meet high load-to-weight ratio and ultra-high-speed operation. In this paper, the H method is used for numerical modeling of superconducting bulk materials in the COMSOL software, and the finite element model is used to establish the external magnetic field. For axial superconducting bearings, there is an optimal size of permanent magnets. The effects of relaxation, preload and radial offset on the suspension force are studied, and the rotor structure is optimized to further increase the maximum speed of the rotor.**

## Keywords

**Axial Superconducting Bearing, Relaxation , Preload, Radial Offset.**

## 1. Introduction

High-temperature Superconducting Magnetic Bearing (SMB) is based on the pinning effect principle of the second type of high-temperature superconductor. It is a passive suspension bearing [1]. It does not need lubrication, has less vibration and noise, and overcomes It eliminates the space instability of permanent magnetic bearings, and does not require the complicated control technology of electromagnetic bearings. It has the static and low-speed stable suspension performance that electric bearings do not have. It can be used in a wide range of environments and can operate in vacuum and low temperature environments. Superconducting bearings are one of the core components of superconducting magnetic levitation flywheel energy storage devices. The important properties of the flywheel such as energy storage, speed and energy storage density are directly related to the bearing.

The axial superconducting bearing structure is relatively simple and convenient to manufacture as shown in Figure 1. Due to the limitation of the residual magnetic flux density of the permanent magnet, it is suitable for applications with small load, and can be used for small flywheel energy storage. Superconducting bearings are currently carrying out more studies on two-dimensional bearing suspension force simulation and time-varying magnetic field losses. At this stage, the trial and error cost of high-speed and heavy-duty superconducting bearing prototypes is relatively high. Simulation calculations can save costs and improve research efficiency. This paper mainly studies the relaxation and preload characteristics of axial high-temperature superconducting bearings, and optimizes the rotor structure to further increase the maximum speed of the rotor.

ISSN: 2664-9640

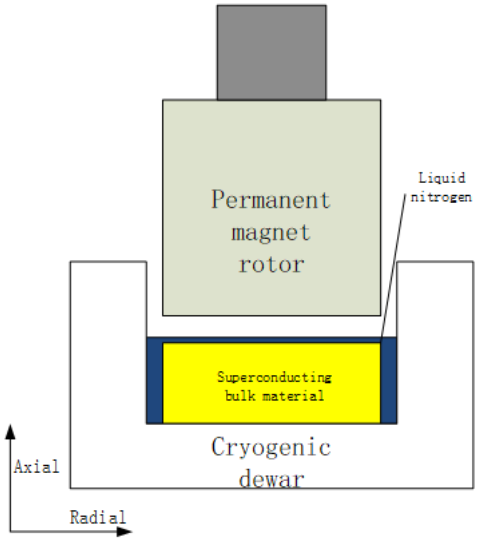


Figure 1: Axial superconducting bearing schematic

## 2. Structural characteristics and optimization

### 2.1. Permanent magnet size selection

Since the axial bearing needs cooling due to the superconducting block material, it is more convenient to make the stator, and the cylindrical permanent magnet is used as the rotor. According to the existing block material in the laboratory is the cylindrical block material of Φ55×13mm, the structure of the permanent magnet is optimized. Experiments show that the use of N52 grade neodymium iron boron permanent magnets for the axial superconducting bearing rotor can provide higher magnetic flux and generate higher induced current in the superconductor. The permanent magnet is modeled by the COMSOL software by defining the residual magnetic flux density of the permanent magnet. This module is calculated by the vector magnetic potential A, and the grid is divided into an unstructured grid to solve the permanent magnet spatial magnetic field distribution in the steady state.

Simulate the permanent magnets of Φ45×45mm, Φ50×50mm, Φ55×55mm, and Φ60×60mm. The movement of the permanent magnet is shown in Figure 2.1(a), (a) the permanent magnet is located 30 mm away from the superconducting block and cooled to liquid nitrogen temperature (b) the permanent magnet is lowered to 5 mm away from the block, and (c) moves The permanent magnet returns to the field cold position 30 mm. The moving speed here is 1 mm/s, in order to show that the superconducting block is on the top and the permanent magnet is on the bottom.

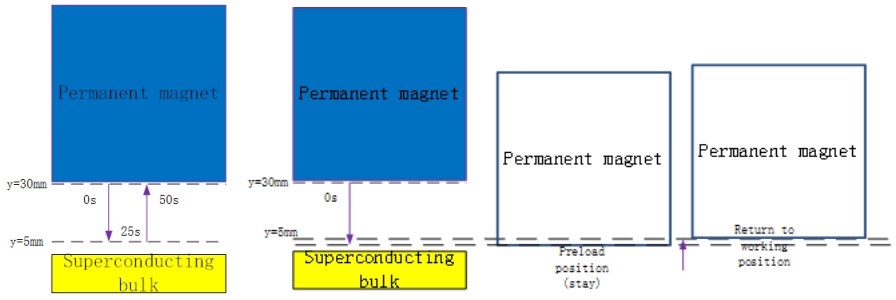


Schematic of permanent magnet test Schematic of preloading process

Figure 2.1: Permanent magnet moving position

ISSN: 2664-9640

It can be seen from Figure 2.2 that the suspension force of different permanent magnet rotors all show obvious hysteresis. When the diameter of the permanent magnet is smaller than the diameter of the superconducting block, the maximum levitation force increases as the diameter of the permanent magnet increases. When the diameter of the rotor is larger than the diameter of the superconducting block, the maximum levitation force decreases. However, the stable suspension of the second type of superconductor is due to the magnetic flux pinning effect. The Meissner effect is a type of superconductor characteristic and cannot fully simulate the current distribution inside the superconductor. This paper uses the H method to show the current distribution inside the block.

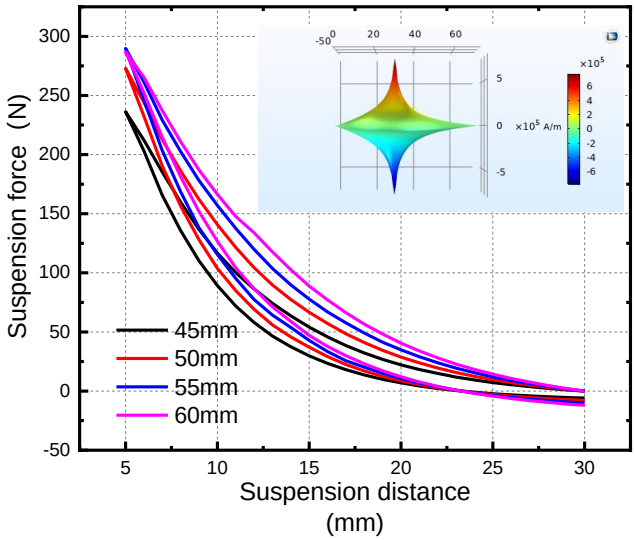


Figure 2.2:Comparison of the suspension force of permanent magnets with different diameters

It can be seen from Table 1 that when the diameter is below 55 mm, the maximum levitation force increases with the increase of the total magnetic energy, but when the diameter exceeds 55 mm, the levitation force decreases slightly. This is because the block material first induces current at the edge and has the largest current density. When the diameter of the permanent magnet rotor exceeds the diameter of the superconducting block material, the maximum magnetic field at the edge of the permanent magnet cannot be fully utilized by the block material, so the suspension force is slightly reduced. Consistent with the conclusion that Meissner's complete diamagnetic effect was adopted in the literature, this paper uses a 55 mm diameter permanent magnet with the same diameter as the superconducting bulk material for relaxation and preload research.

Table 1: Permanent magnet performance comparison

| Permanent magnet diameter | 45mm | 50mm | 55mm | 60mm |
|---|---|---|---|---|
| Maximum suspension force(N) | 236 | 272 | 290 | 286 |
| Total magnetic energy(J) | 20.1 | 28.3 | 38.9 | 52.3 |

## 2.2. Relaxation characteristics

Current relaxation can also reflect the stability of the superconducting system. The smaller the current relaxation, the more stable the system is [2]. Although lowering the operating temperature can effectively inhibit the relaxation of the block material, the cost of liquid helium

ISSN: 2664-9640

cooling for axial superconducting bearings is relatively high, and liquid nitrogen refrigeration cannot effectively reduce the temperature of the block material.

It can be seen from Fugure:2.3(a) that the suspension force stays at this position for 300 s when the working height is 5 mm when the suspension force reaches the maximum. Since the finite element analysis result will have a slight error each time, the suspension force attenuation value is used here. At the end of s calculation, the attenuation value of the suspension force is 27.8 N, which is 9.5%. The illustration shows the relaxation attenuation value of the suspension force in logarithm of time, that is, the attenuation value within the time of ln(t-25); (b) It can be seen that the current density inside the block material (the maximum current density in the display diagram is the absolute value of the current density) gradually decreases, and the decay trend of the suspension force is the same. The current distribution inside the block material is shown in Figure 2.4.

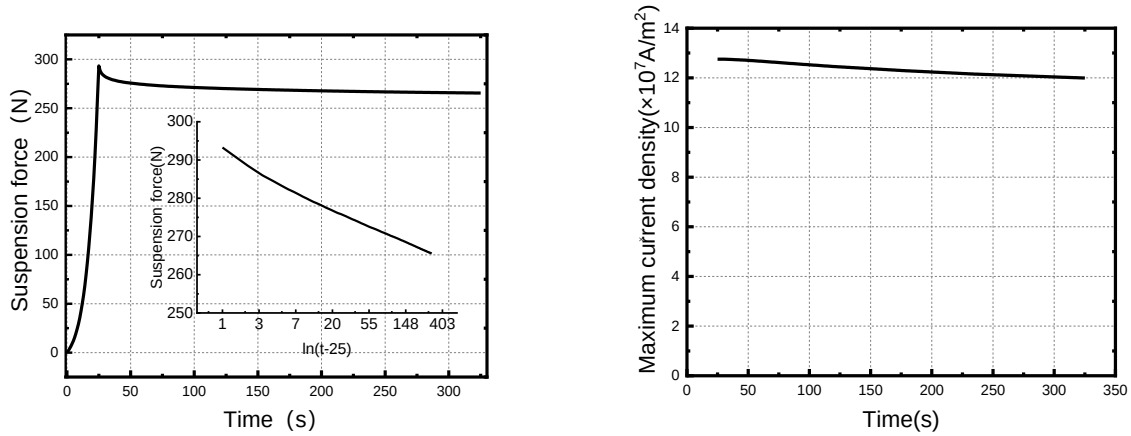


Suspension force Current density

Figure 2.3:300s Relaxation characteristics

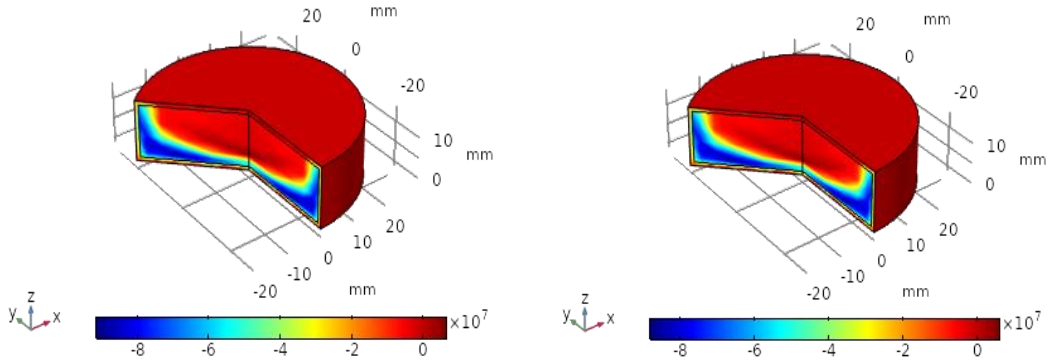


(c) t=125 s (d) t=325 s

Figure 2.4: 300s Relaxation current density distribution cloud map

## 2.3. Preload characteristics

The specific steps of the preloading method are shown in Figure 2.5(b): first lower the superconducting bulk material to 1-2 mm above the working height, and stay for a few seconds to ensure that the induced current inside the bulk material relaxes. After staying for a period of time That is, ascend the bulk material to the working height, and stay at the working position

ISSN: 2664-9640

for 300 s to record the relaxation process of the bulk material suspension force and the current density change.

From Figure 3 10(a), it can be seen that when the preload is 1 mm (the rotor is lowered to 4 mm, which exceeds the working height by 1 mm), the levitation force reaches 326 N. After 100 s of preload, the levitation force is reduced to 301 N. The attenuation value of the suspension force during the loading phase is 25 N, and then the rotor returns to the working height of 5 mm. After 25 s, the suspension force drops to 247.7 N, and then after 25 s, the suspension force drops slightly, basically stable at 244.9 N, and finally at 300 s At the end of relaxation, the levitation force stabilizes at 245.5 N.

It can be seen from Fig. 3 10(b) that when the rotor is lowered to 4 mm, the current density reaches the maximum, after 100 s the relaxation current density continues to decrease, and then the rotor reaches the working height of 5 mm, at this time reverse current is generated inside the block , Offsetting part of the initial current, after 25 s, the current density declines faster, which is the same as the decline trend of the suspension force; the current density continues to decline until the end of the relaxation, but the attenuation is slower than the preload stage.

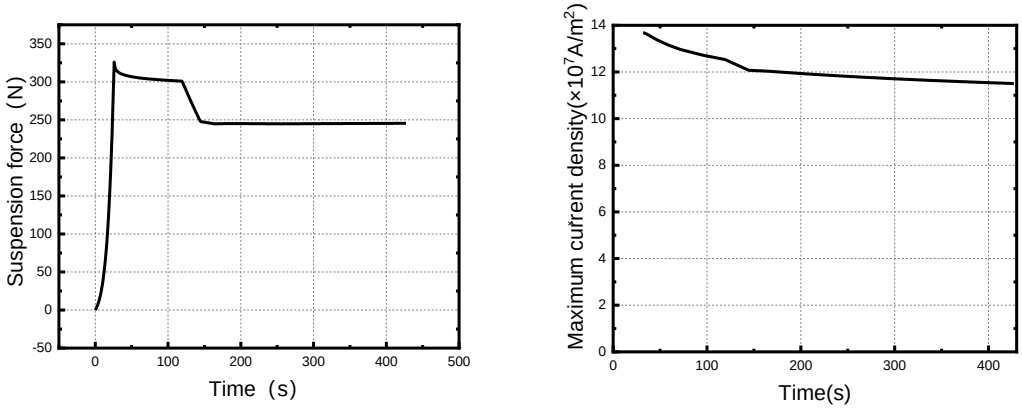


(a) Suspension force (b) Current density

Figure 2.5: 100 s suspension characteristic with 1 mm preload

From the current density distribution cloud diagram in Figure 2.6, it can be seen that when the rotor is lifted to the working height at the end of the preload, a reverse current appears, and then the reverse current continues to increase, spreading from the corner of the block to the bottom. The downward trend is consistent.

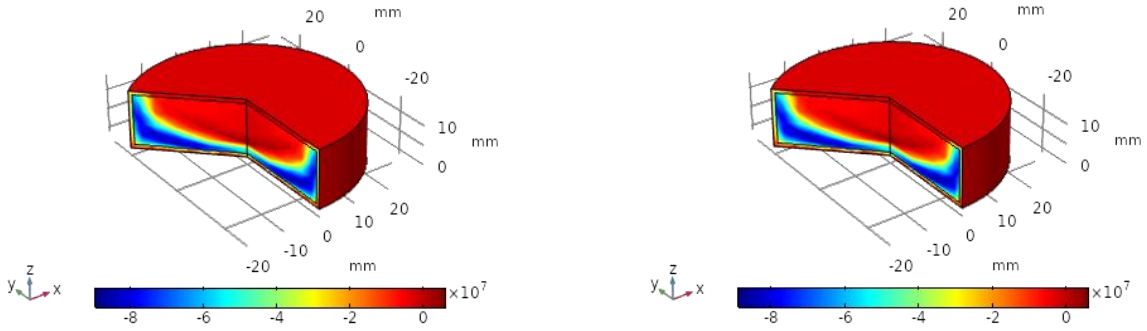


t=125 s t=127 s

ISSN: 2664-9640

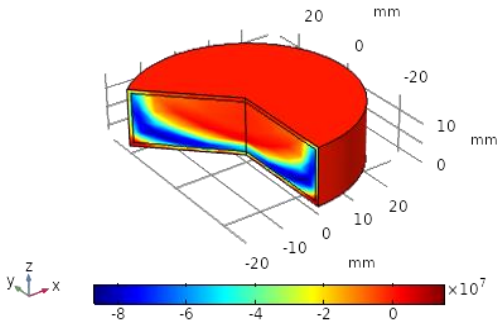


(c) t=157 s

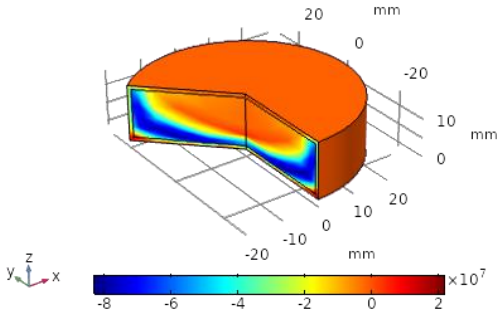


(d) t=427 s

Figure 2.6: Current distribution cloud diagram for 100 s with 1 mm preload

For the preloading process, it can be seen from Table 2 that at different preload distances, the final levitation force will be affected. At different times of 1 mm preload, the final levitation force is basically the same, that is, a reasonable preload time has an effect on the final levitation force. The effect is small. The final suspension force under 2 mm preload is smaller than that under 1 mm preload, that is, the larger the preload distance, the smaller the final suspension force.

Table 2: Comparison of relaxation and preload suspension force

| | 300s relaxation | 3000s relaxation | 1 mm Preload | | 2mm preload 300 s |
|---|---|---|---|---|---|
| | | | 100 s | 300 s | |
| Initial suspension force | 293.3 | 293 | 326 | 326.1 | 363.5 |
| Suspension force after prelod | — | — | 286.1 | 279.4 | 318 |
| Suspension force after relaxation | 265.5 | 256.9 | 245.5 | 245.7 | 223.4 |

## 2.4. Rotor offset characteristics

The block material used in this chapter is cylindrical, and structured grids cannot be directly used. The center part of the block material can be divided into unstructured grids, and the rest can be divided into structured grids. When the axial bearing is running, the stator and the rotor are not on the same axis, that is, the phenomenon of deviation or tilt, or the deviation and tilt occur at the same time.

It can be seen from Figure 2.7(a) that the levitation force is the largest when there is no radial offset between the superconducting stator and the permanent magnet rotor, and when there is a radial offset, the levitation force decreases with the increase of the offset distance, as shown in Figure 2.7(b) It can be seen that when the offset is 5 mm, 10 mm, 15 mm, and 20 mm, the overlapping area of the stator and the rotor decreases linearly, and the downward trend of the suspension force and the overlapping area is basically the same, so when the axis is measured The levitation force when consistent, that is, no offset, can be estimated when the offset is less than 20 mm.

ISSN: 2664-9640

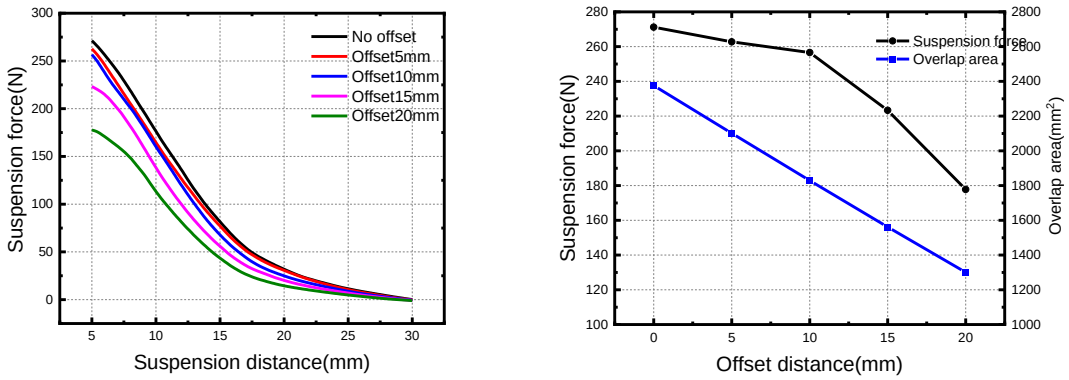


(a) Suspension force curve

(b) Relationship between suspension force and overlap area

Figure 2.7: Rotor offset suspension characteristics

When the radial movement offset distance of the block is different, the downward trend of the suspension force is basically the same. The attenuation value of the suspension force of the block material moving radially from the origin for the first time and returning to the origin point is obviously larger than that of the second time, but the difference decreases with the increase of the offset, that is, a certain offset affects the radial movement of the block material. The attenuation has an inhibitory effect.（Figure2.8）

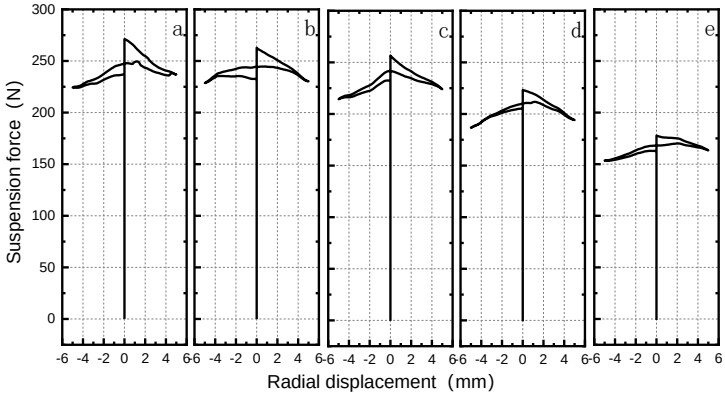


Figure 2.8:Radial displacement suspension characteristics ((a) No offset (b)5 mm (c)10 mm(d)15 mm(e)20 mm)

It can be seen from Table 3that after the block material completes one reciprocation, the attenuation value of the suspension force after movement decreases with the increase of the offset, the attenuation value is 35.3 N when there is no offset, and the attenuation value of the suspension force is 15 when the offset is 20 mm. N, the attenuation value is 42.5% when there is no offset, which also reflects the suppression of the attenuation of the suspension force by the radial offset.

Table 3: Offset suspension force attenuation value

| Offset distance | No offset | 45mm | 50mm | 55mm | 60mm |
|---|---|---|---|---|---|
| Initial suspension force(N) | 272.2 | 262.7 | 256.6 | 223.3 | 177.8 |
| Offset suspension force(N) | 236.9 | 232.2 | 232 | 205.5 | 162.8 |
| Total magnetic energy(J) | 35.3 | 30.5 | 24.6 | 17.8 | 15 |

ISSN: 2664-9640

## 3. Rotating speed optimization

According to the size of the block material, the selected Φ55×55 mm neodymium-iron-boron permanent magnet rotor has a tensile strength of 80 MPa. Since the permanent magnet is a brittle material, the rotor speed of the axial superconducting bearing is higher and the safety factor is S=4. The allowable stress of permanent magnet is only 20 MPa. A sheath made of a material with higher tensile strength is assembled outside the cylindrical surface of the permanent magnet rotor as shown in Figure 3.1(a). Interference press fitting is used between the layers to generate pre-pressure, which can affect the permanent magnet rotor. The protection can also increase the speed of the permanent magnet rotor.

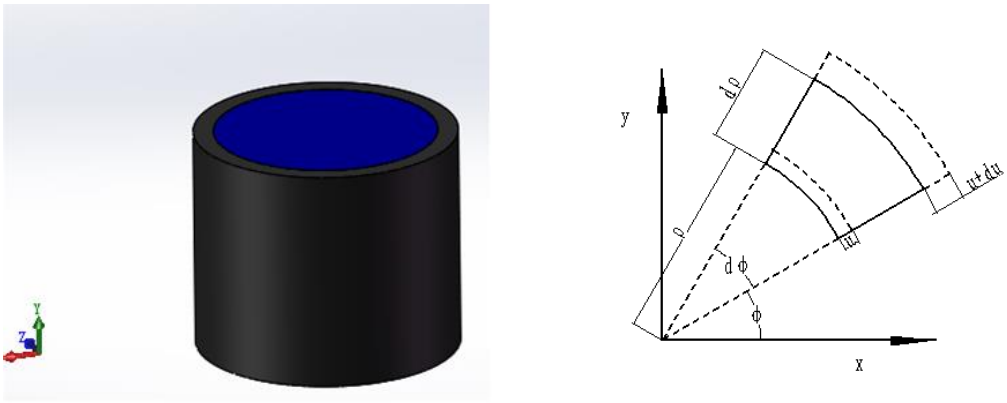


(a)Titanium alloy protective sleeve (b)Stress analysis of equal thickness disc

Figure 3.1:Stress analysis of titanium alloy sheath and equal thickness disc

Only the cylindrical permanent magnet is calculated for stress, and the uniform thickness disk rotating at a uniform angular speed can be used to solve the stress problem as shown in Figure 3.1(b). Taking the radial displacement u as the unknown quantity, the radial strain and the hoop strain are [3]:

$$\left.\begin{aligned}\varepsilon_\rho &= \frac{du}{d\rho}\\ \varepsilon_\theta &= \frac{u}{\rho}\end{aligned}\right\} \tag{3-1}$$

If the angular velocity of the disc is ω, the material density is $\rho_0$, and the inertial force per unit volume is:

$$F_d = \rho_0 \omega^2 \rho \tag{3-2}$$

The $F_d$ direction is along the direction of the coordinate axis ρ, and the D'Alembert principle is used to establish the balance equation to obtain the static balance equation:

$$\frac{d\sigma_\rho}{d\rho} + \frac{\sigma_\rho - \sigma_\varphi}{\rho} + \rho_0 \omega^2 \rho = 0 \tag{3-3}$$

In the case of linear elasticity, from the generalized Hooke's law:

$$\left.\begin{aligned}\varepsilon_\rho &= \frac{1}{E}(\sigma_\rho - \mu\sigma_\varphi)\\ \varepsilon_\varphi &= \frac{1}{E}(\sigma_\varphi - \mu\sigma_\rho)\end{aligned}\right\} \tag{3-4}$$

When the disk is rotating, the radial and circumferential stresses are tensile stresses, and they increase with the decrease of the radius. When the radius is 0, the two Both reach the maximum:

ISSN: 2664-9640

$$(\sigma_\rho)_{\max} = (\sigma_\varphi)_{\max} = \frac{\rho_0(3+\mu)\omega^2 b^2}{8} \tag{3-5}$$

According to the theory of elastic mechanics, the maximum equivalent stress VonMises（$\sigma_{sv}$）:

$$\sigma_{sv} = \sqrt{\frac{1}{2}\left[\sigma_\rho^2 + \sigma_\varphi^2 + \left(\sigma_\varphi - \sigma_\rho\right)^2\right]} \tag{3-6}$$

The solution is ω=2970 rad/s.

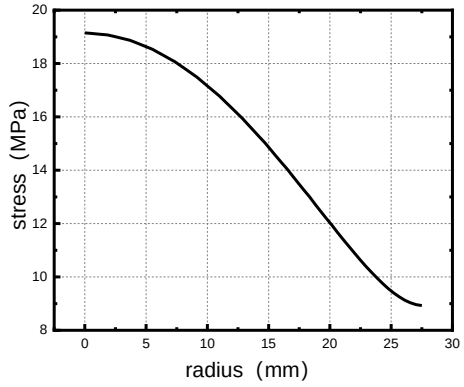


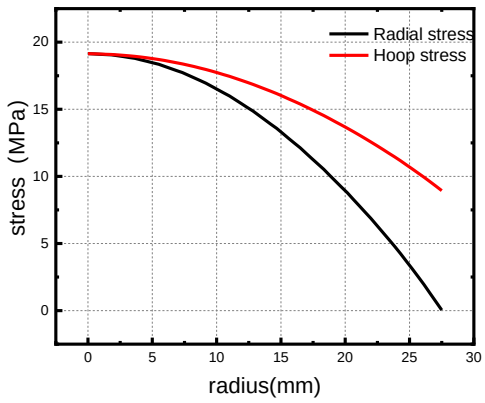


Equivalent stress Circumferential and radial stress

Figure 3.2: Permanent magnet rotor stress

Using finite element calculation, when the rotor speed is 2970 rad/s, the rotor equivalent stress is the largest at the center and smallest at the edge. When the simulation calculation is ω=2970 rad/s, the maximum hoop stress is 19.25 MPa, the maximum radial stress is 19.34 MPa, and the maximum error is 3.75%, which can meet the engineering requirements.(Figure 3.2)

If protection measures are not taken under high-speed rotation, the permanent magnet will be stressed due to inertial force, and the permanent magnet will be destroyed if the stress exceeds the tensile strength. The permanent magnet sheath is made of titanium alloy to ensure that the rotor runs at high speed. The method of assembling the cooling permanent magnet or the heating sheath is used for interference assembly. Considering that the heating sheath temperature is high, the permanent magnet will be demagnetized due to high temperature, and the permanent magnet can be cooled for assembly.

Titanium alloy is an isotropic material. The elastic mechanics theory can be used to deduce the contact stress between the mating surfaces. The contact pressure of the mating surfaces generated by the interference during press-fitting can be derived as follows:

$$P_i = \frac{\delta}{2b} \bullet \frac{1}{\frac{c^2+b^2}{E_1(c^2-b^2)} + \frac{b^2+a^2}{E_2(b^2-a^2)} + \frac{\mu_1}{E_1} - \frac{\mu_2}{E_2}} \tag{3-7}$$

The yield strength of the titanium alloy is 930 MPa, taking 3 times the safety margin, that is, the allowable stress of the sheath is 310 MPa. According to this parameter, the stress under static and high speed is optimized, and the axial force can be ignored.

From Figure 3.3(b), it can be seen that when the interference is below 0.08 mm (under 0 MPa is the internal radial stress of the permanent magnet rotor, above 0 MPa is the equivalent stress in the titanium alloy sheath), the equivalent stress is less than the allowable stress 310 MPa, and the internal radial stress value is negative, at this time the permanent magnet rotor is in a compressed state as shown in Figure 3.3(a). The thickness of the sheath is 5 mm, 10 mm, and

ISSN: 2664-9640

15 mm, and the interference is 0.05 mm and 0.08 mm respectively for speed optimization. The maximum allowable stress of the permanent magnet is 20 MPa.

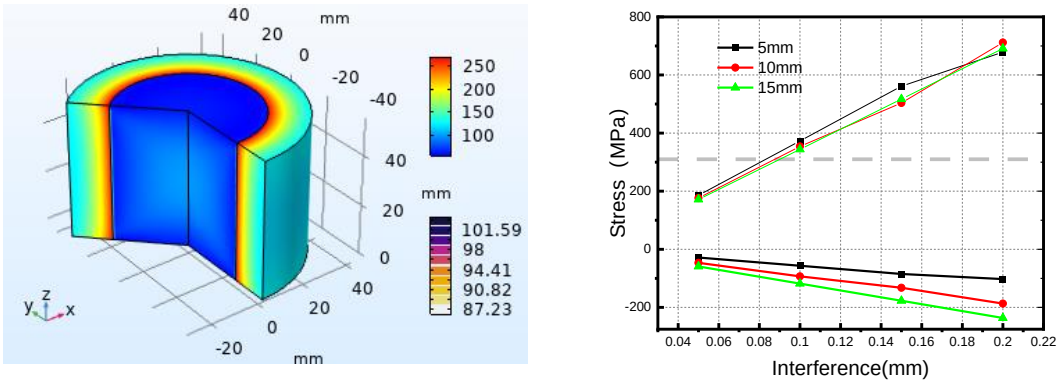


Figure 3.3: Interference and stress characteristics of rotor at rest

It can be seen from Figure 3.4(a) that when the sheath thickness is 5 mm and the interference is 0.05 mm, the maximum speed is 3100 rad/s, which is 4.3% higher than 2970 rad/s without the sheath; Figure 3.4(b) When the sleeve thickness is 5 mm and the interference is 0.08 mm, the maximum speed is 3900 rad/s, which is 31% higher than the case without the sleeve. In this section, the permanent magnet rotor radius of 27.5 mm is the internal radial stress of the permanent magnet, and the outside 27.5 mm is the equivalent stress of the titanium alloy sheath.

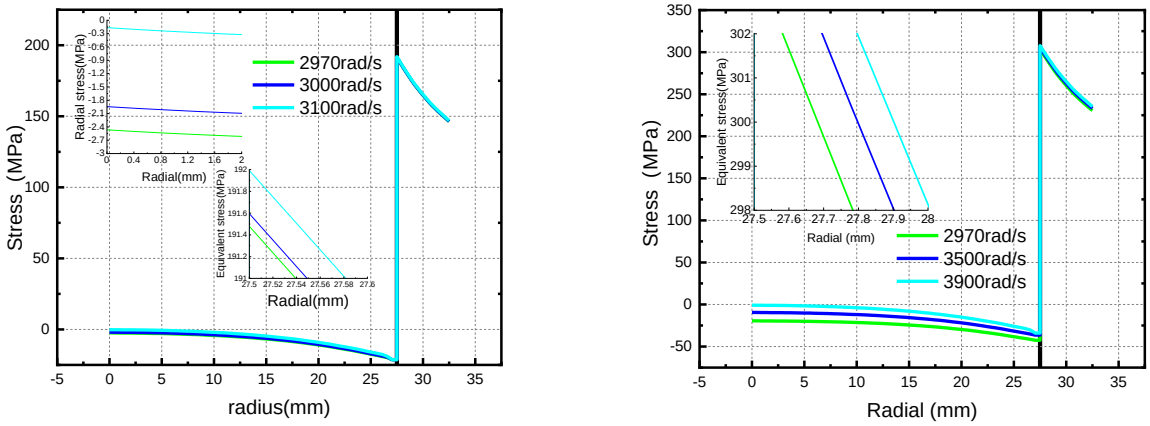


0.05 mm interference 0.08 mm interference

Figure 3.4:5mm thick sheath stress

It can be seen from Table 38 that when the thickness of the sheath is the same, the maximum speed increases significantly when the interference is large. When the interference is the same, the maximum speed increases with the thickness of the sheath, but the maximum speed tends to be saturated when the thickness is increased. When the sheath thickness is 15 mm and the interference is 0.08 mm, the speed is increased by 53.2%. If an anisotropic composite material with higher hoop tensile strength is used as the sheath, the speed can be further increased.

## 4. Conclusion

(1) In the case of using high-performance permanent magnets, when the diameter of the permanent magnet is the same as the diameter of the superconducting block, the greater the axial suspension force, the logarithm of the suspension force and time decreases linearly during

ISSN: 2664-9640

the relaxation of the block. Choosing a reasonable preload distance can significantly inhibit the relaxation and attenuation of the bearing suspension force;

(2) The levitation force can be estimated when the single block has no offset. When the block and the permanent magnet have an inclination angle, the attenuation is small when the block and the permanent magnet are moved laterally, and the levitation force is laterally moved at an orthogonal inclination angle. Greater attenuation;

(3) The permanent magnet rotor adopts titanium alloy as the sheath interference assembly. Selecting the appropriate sheath thickness and interference can increase the speed by 53.2%.

## References

[1] Moon F C, Chang P Z: Applied Physics Letters ,High-speed rotation of magnets on high-Tc superconducting bearings[J]. Vol.56(1990)No.4,p.397-399.

[2] Wei Liu, Suyu Wang, Changqing Ye, ect: Effect of Preloading Process on Relaxation Characteristics of YBCO Bulk Magnet , Journal of Low Temperature Physics, V36(2014) No.01,p.65-69.

[3] Hongwen Liu:.Mechanics of Materials Ⅱ ( Beijing: Higher Education Press ,China 2010),p.170.